ELSEVIER

Physica D 168–169 (2002) 1–9

PHYSICA D

www.elsevier.com/locate/physd

Resonance in periodically inhibited reaction–diffusion systems

Karl Martinez, Anna L. Lin, Reza Kharrazian,
Xaver Sailer, Harry L. Swinney*

Center for Nonlinear Dynamics and Department of Physics, The University of Texas at Austin, Austin, TX 78712, USA

Abstract

We have conducted experiments on a periodically inhibited oscillatory Belousov–Zhabotinsky (BZ) reaction–diffusion system in a regime in which the patterns oscillate at half the frequency of the forcing (the 2:1 resonance regime). The periodic perturbations of the photosensitive (ruthenium-catalyzed) reaction are made with light, which inhibits the oscillatory behavior. Increasing the light intensity increases the refractory period (time for recovery from inhibition), which decreases the oscillation frequency of the patterns in the medium. We investigate the behavior for two different levels of inhibitor concentration in the reagent feed to determine the shape of the 2:1 resonant regime as a function of the forcing intensity and forcing frequency. At high forcing intensity, the inhibition leads to a transition from traveling waves (spirals) to standing waves. Simulations of a reaction–diffusion model with FitzHugh–Nagumo kinetics yield behavior similar to that observed in the experiments.

PACS: 82.40.Bj; 82.40.Ck; 82.20.−w; 89.75.Kd

Keywords: Belousov–Zhabotinsky reaction; Periodic forcing; Reaction–diffusion; Resonance

1. Introduction

The effect of inhibitory stimuli [1–3] on oscillatory behavior has been studied in biological systems such as cardiac muscle cells [4] and networks of nerve cells [5,6]. We examine the effect of an inhibitory stimulus on the ruthenium-catalyzed Belousov–Zhabotinsky (BZ) reaction–diffusion system, where the inhibition is produced by illumination with visible light [7]. The light-sensitive BZ reaction has been used in previous studies of resonant entrainment of spiral tips [8–12], pattern formation in systems controlled via global feedback [3,13], stochastic resonance [14,15], spiral breakup [16], and wavesplitting [17].

In the BZ reaction, the increased inhibitor concentration produced by illumination of the reacting medium increases the refractory period of the medium (the time the system needs to recover after it is stimulated), and as a result decreases the oscillation frequency [18]. We examine the effect of periodic perturbations for two different sets of chemical conditions, one that has low concentration of inhibitor in the reagents fed to the reactor; this results in high frequency rotating spirals, while a high concentration of inhibitor in the reagent feed results in low frequency rotating spiral patterns. We will refer to the former case as weakly inhibited and the latter case as strongly inhibited.

We perturb the light-sensitive oscillatory reaction with spatially uniform light that is modulated periodically in time. The reaction occurs in a porous membrane. This system, oscillating with frequency

* Corresponding author. Fax: +1-512-471-1558.
E-mail address: swinney@chaos.ph.utexas.edu (H.L. Swinney).

0167-2789/02/$ – see front matter
PII: S0167-2789(02)00490-6

f_R, can lock to the forcing frequency f_F in rational ratios of $f_F:f_R$ [2,3,19]. We observe a tongue-shaped 2:1 resonant regime as a function of the forcing intensity and frequency, and we compare the behavior observed for the two different levels of inhibitor feed concentrations. We find that the level of inhibitor concentration in the ruthenium-catalyzed BZ reaction plays an important role in determining the shape of the locked $f_F:f_R$ entrainment bands [20], which are analogous to the Arnol'd tongues of a forced single nonlinear oscillator [21].

In Section 2, we describe the experimental system and data analysis. Section 3 describes how inhibition produced with light affects the reaction. Section 4 presents observations of the 2:1 resonance tongues for both the weakly inhibited and strongly inhibited systems. Section 5 presents simulations of a reaction–diffusion model with FitzHugh–Nagumo (FN) kinetics, and compares the results of the simulations to the experimental observations. The conclusions are presented in Section 6.

2. Experiment

Our experiment used a stirred continuous flow reactor [2,18,20,22], as shown schematically in Fig. 1. In the reactor a thin, porous Vycor glass membrane separated two reservoirs that contain the different BZ reagents. The average pore size in the membrane was 10 nm, permitting reagents to diffuse through the membrane where the reaction takes place, while preventing large scale convective motion. Magnetic stirring bars at the bottom of each reservoir provided mixing, allowing a homogeneous exchange of reagents at the membrane surfaces.

The patterns that formed in the membrane were detected by measuring the transmission of light through the reacting medium using a time-independent spatially uniform low intensity light source (45 W/m^2). Light transmitted through the membrane was detected with a CCD camera. The camera input was bandpass filtered at 451 nm (filter width 18 nm), which is in the middle of the absorption band of the reduced catalyst, Ru(II). Regions of high Ru(II) concentration absorbed light and appeared dark in our gray scale images. The ruthenium in reservoir II was in the oxidized state, allowing transmission of the imaging light through the solution. Images were recorded every 2 s.

In the absence of forcing, the reaction in the membrane formed rotating spiral patterns of Ru(II) concentration. The fronts from two spirals annihilated when they collided, a characteristic of excitable media with a refractory period. For the conditions studied in this paper, we always observed oscillatory behavior because imperfections in the membrane or at the

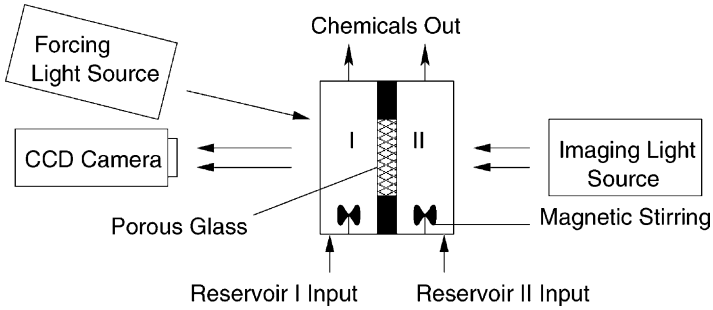

Fig. 1. Schematic diagram of the experiment (not to scale). The BZ reagents from two reservoirs (I, II) diffused into a porous Vycor glass membrane (0.4 mm thick, 22 mm diameter) sandwiched between the two reservoirs. The reaction–diffusion patterns formed in the porous glass. In this study, the pattern wavelength was much larger than the thickness of the thin layer in the porous glass where the patterns formed, so the patterns were quasi-two-dimensional. The reactor was periodically perturbed using spatially homogeneous light from a video projector. The reservoirs, each 8.3 ml in volume, were refreshed at a constant rate (20 ml/h for reservoir I, 5 ml/h for reservoir II). Concentrations of bromate ($[BrO_3^-]$) and bromomalonic acid ([BrMA]) in reservoir I were varied during experiments. The other concentrations were fixed: in reservoir I, 0.80 M sulfuric acid; in reservoir II, 0.18 M potassium bromate, 1×10^{-3} M Tris(2,2'-bipyridyl)dichlororuthenium(II)hexahydrate, and 0.80 M sulfuric acid. All experiments were performed at room temperature.

boundaries acted as pacemakers. The frequency and wavelength of the unforced spiral waves depended on the concentrations of the reagents in the two reservoirs [18,23].

The light-sensitive reaction was forced using blue light from a Sanyo 3LCP video projector. The intensity and spatial homogeneity of the light were computer-controlled using the projector's liquid crystal display. To produce spatially homogeneous illumination, the intensity of each pixel was adjusted until the light reflected from a gray card was spatially uniform [18]. The intensity of the forcing light was continuously monitored using a photodiode. The periodic forcing experiments were conducted with square wave modulation of the light intensity, obtained by blocking the light (intensity γ^2) during half of each forcing period ($1/f_F$).

To determine if a pattern in the membrane was frequency locked, we calculated the power spectrum of the time series for each pixel in a 100×100 array (a $9\,\text{mm} \times 9\,\text{mm}$ area of the membrane). The signal-to-noise of the time series from an individual pixel was too low to diagnose phase locking from the phase information. The 10,000 power spectra were summed, and the pattern's primary response frequency (f_R) was determined from the summed spectrum. Patterns were designated 2:1 frequency locked when the ratio f_F/f_R was 2.0 ± 0.1.

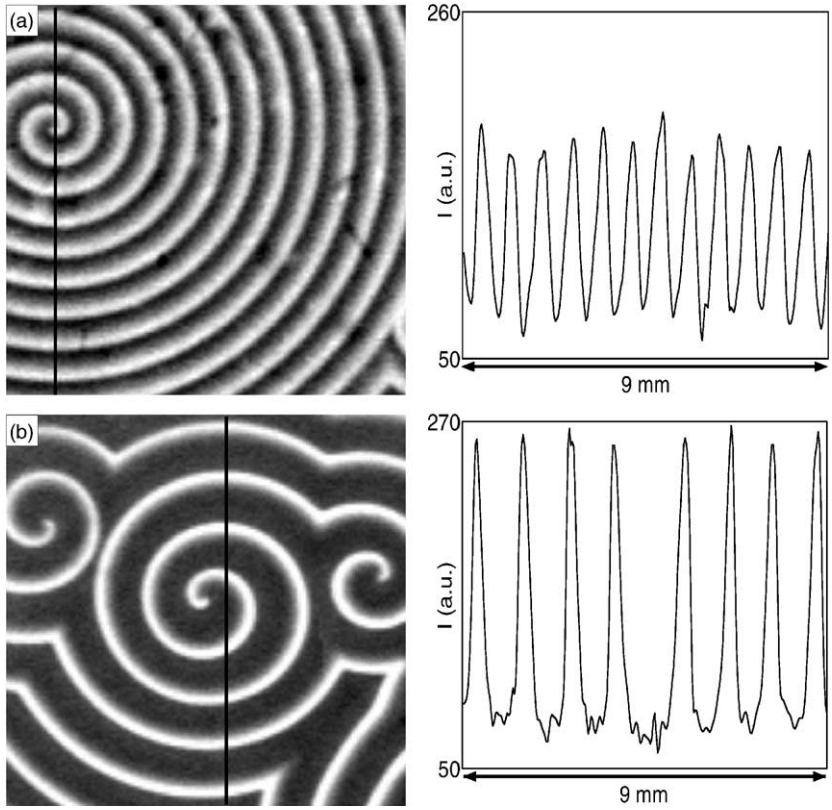

Fig. 2. Unforced spiral patterns under different chemical conditions. (a) Spiral waves with a short refractory period (weakly inhibited medium), $[\text{BrMA}] = 0.220\,\text{M}$, $[\text{BrO}_3^-] = 0.230\,\text{M}$, $\iota \equiv [\text{BrMA}]/[\text{BrO}_3^-] = 0.96$. (b) Spiral waves with a long refractory period (strongly inhibited medium), $[\text{BrMA}] = 0.300\,\text{M}$, $[\text{BrO}_3^-] = 0.136\,\text{M}$, $\iota = 2.2$. The images on the left show a $9\,\text{mm} \times 9\,\text{mm}$ region of the pattern, and the graphs on the right show the intensity as a function of position along the black line through each image on the left. White regions in the images correspond to low concentrations of Ru(II), or excitation fronts. Dark regions correspond to high concentrations of Ru(II) where the medium is in a non-excited or refractory state.

3. Inhibition in the BZ reaction

In this section, we first discuss the effect of varying chemical concentrations on the spiral frequency of the unforced BZ system. Then we show how forcing with light alters spiral behavior.

3.1. Chemical dynamics

In the BZ reaction, ruthenium catalyzes the oxidation of bromate, forming bromous acid in the presence of sulfuric acid and malonic acid. The production of bromous acid leads to further oxidation of bromate in the system [24], and Ru(II) is converted to Ru(III) during this auto-catalytic process. In a spatially extended BZ medium of high Ru(II) concentration, self-propagating waves of rapidly increased levels of Ru(III) form fronts of auto-catalysis (excitation fronts). An excitation results in a rapid increase in the concentration of the inhibitor Br^- beyond a critical threshold. Another wave of auto-catalytic activity cannot be initiated until the $[Br^-]$ falls below the inhibition threshold. The refractory period is the time between the excitation of a front and the later return of inhibitor concentration to below the threshold value.

Examples of unforced spirals corresponding to weakly inhibited and strongly inhibited chemical kinetics are shown in Fig. 2. The frequency f_S of unforced stable rotating spirals is shown in Fig. 3 for varying concentrations of bromate and bromomalonic acid (the source of Br^-, the inhibitor) in reservoir I. A measure of the inhibition is given by the concentration ratio $\iota \equiv [\mathrm{BrMA}]/[\mathrm{BrO_3^-}]$. For the weakly inhibited system, $\iota = 0.96$, spirals of high frequency

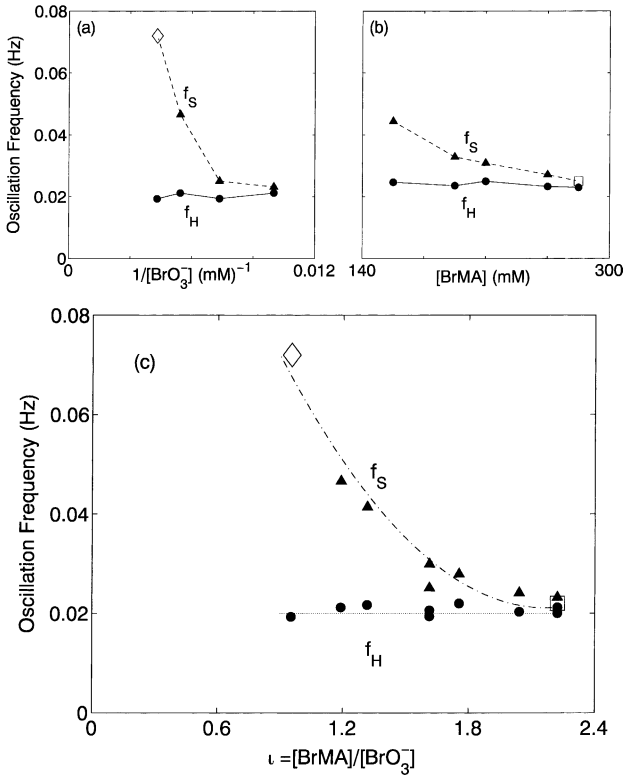

Fig. 3. Oscillation frequencies measured for the spatially homogeneous system, f_H (●), and for spirals in the absence of light forcing, f_S (▲), as a function of (a) $1/[\mathrm{BrO_3^-}]$ and (b) [BrMA], in reservoir I. The dependence of the frequencies on the concentration ratio, $\iota \equiv [\mathrm{BrMA}]/[\mathrm{BrO_3^-}]$, is shown in (c). The symbols ◇ and □ correspond respectively to the weakly inhibited and strongly inhibited spirals shown in Fig. 2. In (a) [BrMA] was fixed at 220 mM; in (b) $[\mathrm{BrO_3^-}]$ was fixed at 184 mM.

(0.072 Hz) form with a sinusoidal wave profile, as shown in Fig. 2(a). The unforced spiral frequency f_S decreases (see Fig. 3) and the spiral wave profile becomes relaxational with a higher concentration of the inhibitor source (BrMA), or a lower concentration of the activator species (BrO_3^-). Fig. 2(b) is an example of a strongly inhibited spiral, $\iota = 2.2$. The medium is so strongly inhibited for $\iota > 2.3$ that it no longer oscillates; spirals do not form in the membrane.

3.2. Effect of light

The effect of light is well understood for the ruthenium-catalyzed BZ reaction in a homogeneous (well-stirred) reactor [7]: light in the absorption band centered at 450 nm increases the release of free bromide, which inhibits the reaction. Increased illumination intensity lowers the frequency of oscillation because of the longer refractory period between excitations. At a critical illumination intensity, all excitations are inhibited and oscillations cease.

We determined the effect of light on both the underlying homogeneous frequency of the spatially extended system and on the frequency of the rotating spiral pattern. To determine the oscillation frequency of the homogeneous medium, the spiral pattern is annihilated (inhibited) with a high intensity light pulse (30 s duration), which results in a refractory period so long that the spirals cannot propagate. Thus all points in space are phase synchronized in the same inhibited chemical state. After the light pulse is turned off, phase-synchronized (homogeneous) oscillations emerge. Our measurements of the frequency f_H of these homogeneous oscillations are shown in Fig. 3 for different concentrations of [BrMA] and $[BrO_3^-]$. For the chemical concentrations used in our experiments, the frequency f_H (0.02 Hz) is found to be independent of the concentration of bromate and bromomalonic acid.

In a spatially extended excitable medium, the structure with the highest frequency is dominant; hence no spiral can form at a frequency lower than the homogeneous frequency f_H of the medium. At a sufficiently high static forcing intensity, the spiral frequency is reduced to that of the homogeneous oscillation frequency. This explains the observed limiting value of f_S, which is key to understanding the effect of inhibition on the tongue-shaped resonant regimes, as discussed in the following section. The effect of static, time-independent forcing is shown in Fig. 4

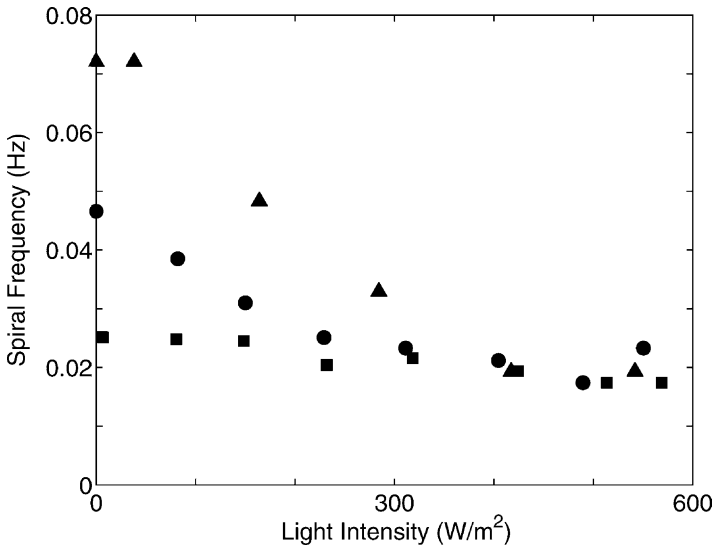

Fig. 4. Spiral frequency as a function of static (time-independent) light intensity for different chemical concentrations $\iota \equiv [BrMA]/[BrO_3^-]$: (▲) $\iota = 0.95$ (weakly inhibited), (●) $\iota = 1.20$, (■) $\iota = 2.20$ (strongly inhibited). The other chemical conditions are given in the caption of Fig. 1.

for three different sets of chemical concentrations in reservoir I. Increasing the light intensity can be seen to inhibit the reaction in the same way as increasing $\iota \equiv [\mathrm{BrMA}]/[\mathrm{BrO_3^-}]$. For all three chemical concentrations, as the light intensity increases, the spiral frequency decreases until it reaches the homogeneous oscillation frequency, 0.02 Hz.

4. Shape of the 2:1 resonance tongue

The Arnol'd type tongue structures in the control parameter space of forcing intensity γ^2 and frequency f_F are shown in Fig. 5 for both the weakly and strongly inhibited chemical kinetics. Points inside the tongues are classified as 2:1 locked with the forcing (as described in Section 2), while points outside the tongues are either not locked or are locked at another resonance. Patterns at the bottom of both tongues have traveling fronts, like the rotating spirals shown in Fig. 2, which propagate one full spiral wavelength for every two forcing cycles. At high intensity forcing ($\gamma^2 > 300\,\mathrm{W/m^2}$), the patterns have stationary fronts separating two locked phase domains which oscillate once during every two forcing cycles. The transition from spiral patterns to standing patterns with increasing forcing intensity was described in our previous study [20]. In neither the strongly nor weakly inhibited systems do we observe complete inhibition of natural oscillations (even at maximum forcing) as has been observed in forced Raleigh–Benard convection [25].

For the weakly inhibited kinetics, the tongue bends to higher frequencies with decreasing forcing, as Fig. 5(a) illustrates, while for the strongly inhibited kinetics the tongue does not bend as much with decreasing forcing, as Fig. 5(b) illustrates. The reason for the difference in the shapes of the tongues for the strongly and weakly inhibited systems can be understood from our measurements of the effect of time-independent forcing (Fig. 4). With static forcing, the spiral frequency f_S approaches the homogeneous frequency f_H as the forcing intensity is increased (see Fig. 4). As the forcing intensity increases, the level of inhibitor rises, increasing the refractory period and thus decreasing maximum spiral frequency that is sus-

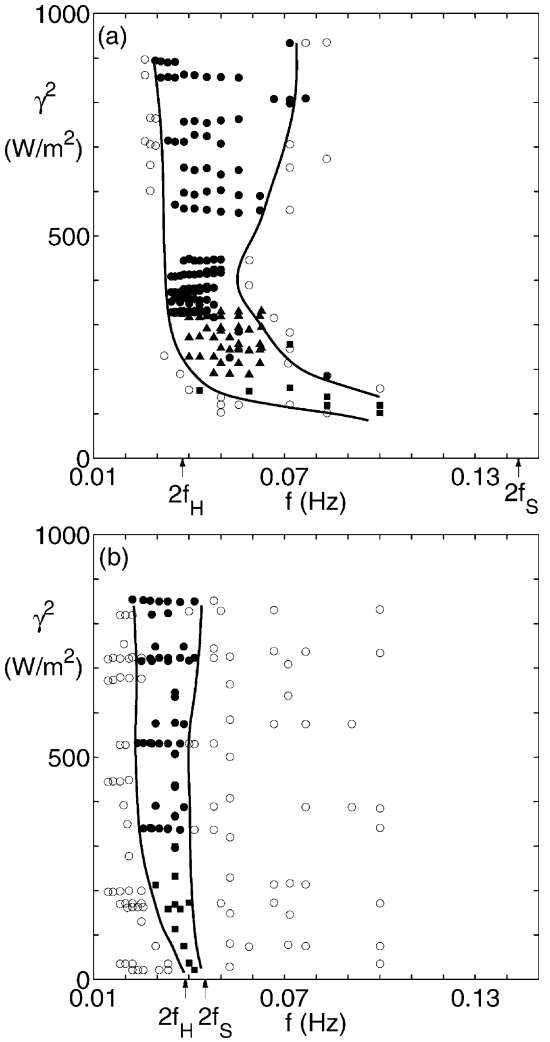

Fig. 5. 2:1 resonant tongues in the forcing frequency–intensity parameter space for (a) weakly inhibited and (b) strongly inhibited kinetics of the BZ system. The reactor was forced using square pulses of light of intensity γ^2 and frequency f_F. Points within the solid curves represent patterns that oscillate at one-half the forcing frequency, while the open circles outside the solid curves correspond to non-2:1 resonant patterns: (■) traveling front patterns; (●) standing wave patterns with stationary fronts; (▲) hybrid patterns with both traveling and standing behavior (see [20]). The arrow on the frequency axes labeled $2f_\mathrm{H}$ is twice the homogeneous oscillation frequency; $2f_\mathrm{S}$ is twice the unforced spiral frequency. Chemical concentrations: (a) $[\mathrm{BrO_3^-}] = 0.230$ M, [BrMA] = 0.220 M, $\iota = 0.96$, $f_\mathrm{H} = 0.019$ Hz, and $f_\mathrm{S} = 0.072$ Hz. (b) $[\mathrm{BrO_3^-}] = 0.136$ M, [BrMA] = 0.300 M, $\iota = 2.22$, $f_\mathrm{H} = 0.019$ Hz, and $f_\mathrm{S} = 0.022$ Hz. The other chemical conditions are given in the caption of Fig. 1.

tained by the medium. Above a static forcing intensity of approximately 300 W/m^2, $f_S \approx f_H$, and increasing γ^2 above this value has no further effect on f_S.

Now consider the periodically forced system. For $\gamma^2 > 300\,\mathrm{W/m^2}$, $f_S \approx f_H$; hence the tongues are approximately vertical for high forcing intensity. But for the weakly inhibited system with $\gamma^2 < 300\,\mathrm{W/m^2}$, the increase in spiral frequency with decreasing forcing intensity leads to a bending of the tongue to higher frequencies, as Fig. 5(a) illustrates. In contrast, in the strongly inhibited system the spiral frequency does not change much with decreasing forcing intensity; hence the tongue does not bend significantly to higher frequencies for the strongly inhibited system (Fig. 5(b)).

5. 2:1 resonance in the FN model

The experiments we have described indicate that periodic inhibition of the oscillatory chemical medium increases the refractory period which dictates the resonant tongue shape in the γ^2–f_F parameter space. We have found similar behavior in a periodically forced reaction–diffusion model with FN kinetics [26–28],

$$\frac{\partial u}{\partial t} = u - u^3 - \left[v - \frac{b}{2}(1 + \cos(2\pi f t))\right] + \delta_1 \nabla^2 u,$$
$$\frac{\partial v}{\partial t} = \epsilon \left\{u - a_1 \left[v + \frac{b}{2}(1 + \cos(2\pi f t))\right] - a_0\right\} + \delta_2 \nabla^2 v, \quad (1)$$

where u and v are the dynamical field variables. The forcing has been chosen to have opposite signs for the variables u and v. In our numerical simulations, we vary the forcing strength b and forcing frequency f, while the other parameters are held fixed: $a_0 = 0.1$, $a_1 = 0.5$, $\epsilon = 0.05$, $\delta_1 = 0.333$, and $\delta_2 = 0.067$.

To understand the effect of forcing on the dynamics of the model, consider first the spatially homogeneous case where $\delta_1 = \delta_2 = 0$. The nullclines $v_1(u)$ and $v_2(u)$ in Fig. 6 are then obtained by solving $\partial u/\partial t = 0$ and $\partial v/\partial t = 0$, respectively. The intersection of the two nullclines, the solution where the rate of change of both u and v is zero, is the fixed point (steady-state) of the system. Only one fixed point is possible when $0 < a_1 \leq 1$. The stability of the fixed point depends on the relative position of the

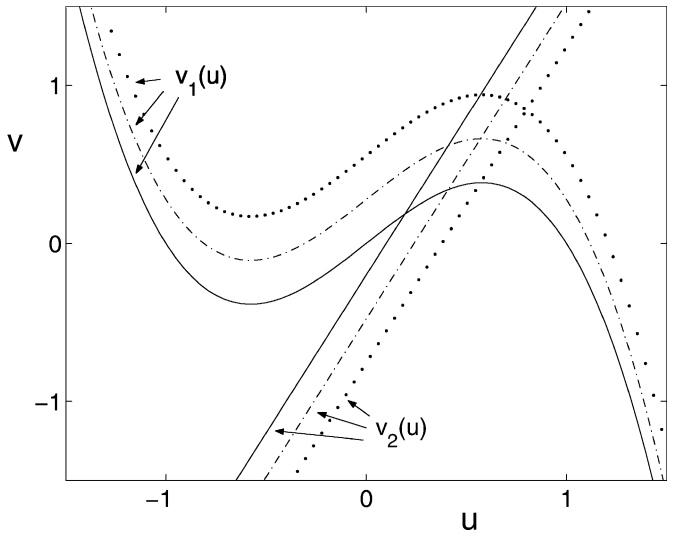

Fig. 6. Nullclines $v_1(u)$, when $\partial u/\partial t = 0$, and $v_2(u)$, $\partial v/\partial t = 0$, of the spatially homogeneous FN model at three different forcing amplitudes b: 0, b_{Hopf} and $2b_{\mathrm{Hopf}}$. The intersection of the nullclines is the fixed point of the system. The intersection of the solid nullclines at the minimum forcing value ($b = 0$) is an unstable fixed point with limit cycle behavior. The dashed-dotted nullclines ($b = b_{\mathrm{Hopf}}$) is at the Hopf-bifurcation point, while intersection of the dotted nullclines ($b = 2b_{\mathrm{Hopf}}$) is a stable fixed point. Parameter values are given in the text.

nullclines, which changes as a function of the periodic forcing.

For our choice of model parameters, the steady-state behavior of the unforced system (intersection of solid lines) is an unstable focus with limit cycle behavior. With the forcing amplitude $0 < b \leq b_{\mathrm{Hopf}}(0.278)$, the fixed point is always an unstable focus with limit cycle behavior. Forcing the system with amplitudes $b > b_{\mathrm{Hopf}}$ periodically shifts the nullclines such that the unstable focus becomes a stable fixed point (intersection of dotted lines) after traveling through a Hopf bifurcation (intersection of dashed-dotted lines), as shown in Fig. 6. The choice of $\epsilon \ll 1$ ensures that the dynamics become excitable as soon as the steady-state becomes stable. This corresponds to the inhibited state of the experiment. In this way, the forced FN system models the periodic inhibition of the BZ system periodically forced with light.

We chose a value of the ratio of the diffusion coefficients δ_1/δ_2 so that spiral patterns in the simulations were similar to the unforced spiral patterns observed in the BZ experiment. Eq. (1) was evaluated on a 256×256 grid with a 150×150 dimensionless domain size and reflective boundary conditions. We used a 5th order Runge–Kutta integration method for the reaction terms and a Crank–Nicholson scheme for the spatial diffusion. A spiral pattern was the initial condition.

The 2:1 resonant tongue for Eq. (1) is shown in Fig. 7 for a particular set of model parameters. Frequency locking behavior was determined from power spectra of time series of grid points in the images, just as in the analysis of the experiments. As observed in the experiments, standing front patterns form in the top portion of the tongue (for $b > b_{\mathrm{Hopf}}$), and traveling spiral patterns were found in the bottom portion of the tongue (for $b < b_{\mathrm{Hopf}}$). At forcing strengths near b_{Hopf} on the high frequency side of the tongue, we observed patterns with mixed traveling and standing behavior, similar to those observed in the weakly inhibited tongue in Fig. 5(a).

Arrows labeled $2f_{\mathrm{H}}$ and $2f_{\mathrm{S}}$ in Fig. 7 point to twice the homogeneous frequency and twice the spiral frequency of the system. The FN tongue is locked around $2f_{\mathrm{H}}$ at high forcing strength and bends toward $2f_{\mathrm{S}}$ as the forcing strength is decreased, which is the same trend that we observed in the experimental tongues.

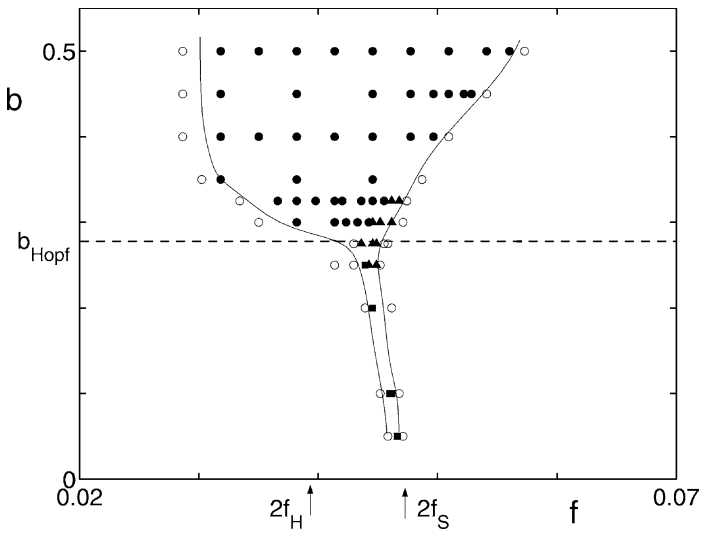

Fig. 7. The 2:1 Arnol'd type tongue for the FN reaction–diffusion model as a function of forcing strength b and forcing frequency f (parameter values: $a_0 = 0.1$, $a_1 = 0.5$, $\epsilon = 0.05$, $\delta_1 = 0.333$, and $\delta_2 = 0.067$). Points within the solid curves represent patterns that oscillate at one-half the forcing frequency, while the open circles outside the solid curves correspond to non-2:1 resonant patterns: (■) are rotating spirals, (●) are two-phase patterns with standing fronts, and (▲) are patterns with both standing and traveling behavior [20]. The natural frequency of the spatially homogeneous system is $f_{\mathrm{H}} = 0.0198$, and the frequency of the unforced spiral is $f_{\mathrm{S}} = 0.0234$. The dashed line identifies the forcing amplitude at which the system reaches the Hopf bifurcation ($b_{\mathrm{Hopf}} = 0.278$).

In both the experimental and FN systems, the shape of a resonant tongue is determined by the difference between f_S and f_H. In the experimental system, we modify the tongue shape by changing inhibitor feed concentration, which alters f_S while f_H remains constant. We varied parameter values in the FN model with no success in changing f_S relative to f_H, but our search in parameter space was limited by the long computational times required for each parameter set. For the parameter values examined, we were not able to obtain an FN tongue as sharply bent as the experimentally observed tongue in Fig. 5(a).

6. Conclusions

Our study of resonance in oscillatory reaction–diffusion media has revealed a connection between inhibition and the shape of the 2:1 resonant tongue. As the strength of inhibitory forcing of the spatially extended BZ reaction is increased, the refractory period of the chemical medium lengthens. A longer refractory period corresponds to a lower oscillation frequency of the system. As a result, the 2:1 resonant tongues from the experiment bend from the higher unforced spiral frequency toward the lower homogeneous oscillation frequency of the system as the forcing intensity is increased. Periodic forcing of the FN model also results in increasing refractory period with increasing forcing intensity. Further, strong forcing of the FN system inhibits front propagation, yielding stationary patterns, as observed in the experiment.

Acknowledgements

We thank G. Carey and A. Ardelea for help with the numerical simulations, and Qi Ouyang and W.D. McCormick for many useful discussions concerning the experiment. This research was supported by the Engineering Research Program of the Office of Basic Energy Sciences of the Department of Energy and the Robert A. Welch Foundation.

References

[1] D. Golomb, G.B. Ermentrout, Phys. Rev. Lett. 86 (2001) 4179.
[2] V. Petrov, Q. Ouyang, H.L. Swinney, Nature 388 (1997) 655.
[3] V.K. Vanag, A.M. Zhabotinsky, I.R. Epstein, Phys. Rev. Lett. 86 (2001) 552.
[4] D.R. Chialvo, J. Jalife, Nature 330 (1987) 749.
[5] V.N. Murthy, E.E. Fetz, Proc. Natl. Acad. Sci. USA 89 (1992) 5670.
[6] C.M. Gray, P. König, A.K. Engel, W. Singer, Nature 338 (1989) 334.
[7] S. Kadar, T. Amemiya, K. Showalter, J. Phys. Chem. A 101 (1997) 8200.
[8] M. Braune, H. Engel, Chem. Phys. Lett. 211 (1993) 534.
[9] O. Steinbock, V. Zykov, S.C. Müller, Nature 366 (1993) 322.
[10] R.-M. Mantel, D. Barkley, Phys. Rev. E. 54 (1996) 4791.
[11] A. Karma, V. Zykov, Phys. Rev. Lett. 83 (1999) 2453.
[12] V. Hakim, A. Karma, Phys. Rev. E 60 (1999) 5073.
[13] V.K. Vanag, L. Yang, M. Dolnik, A.M. Zhabotinsky, I.R. Epstein, Nature 406 (2000) 389.
[14] S. Kadar, J. Wang, K. Showalter, Nature 391 (1998) 770.
[15] I. Sendiña-Nadal, E. Mihaliuk, J. Wang, V. Pérez-Muñuzuri, K. Showalter, Phys. Rev. Lett. 86 (2001) 1646.
[16] M. Markus, G. Kloss, I. Kusch, Nature 371 (1994) 402.
[17] A.P. Muñuzuri, V. Pérez-Villar, M. Markus, Phys. Rev. Lett. 79 (1997) 1941.
[18] V. Petrov, Q. Ouyang, G. Li, H.L. Swinney, J. Phys. Chem. 100 (1996) 18992.
[19] L. Glass, Nature 410 (2001) 277.
[20] A.L. Lin, M. Bertram, K. Martinez, H.L. Swinney, A. Ardelea, G.F. Carey, Phys. Rev. Lett. 84 (2000) 4240.
[21] J. Glazier, A. Libchaber, IEEE Trans. Circ. Syst. 35 (1988) 790.
[22] Q. Ouyang, R. Li, G. Li, H.L. Swinney, J. Chem. Phys. 102 (1995) 2551.
[23] A. Belmonte, Q. Ouyang, J.M. Flesselles, J. Phys. II France 7 (1997) 1425.
[24] R. Field, E. Koros, R. Noyes, J. Am. Chem. Soc. 94 (1972) 8649.
[25] A. Chiffaudel, S. Fauve, Phys. Rev. A 35 (1987) 4004.
[26] M. Bär, M. Eiswirth, Phys. Rev. E 48 (1993) 1635.
[27] P. Jung, A. Cornell-Bell, F. Moss, S. Kadar, J. Wang, K. Showalter, Chaos 8 (1998) 567.
[28] A.L. Lin, A. Hagberg, A. Ardelea, M. Bertram, H.L. Swinney, E. Meron, Phys. Rev. E 62 (2000) 3790.